

Compressibility as a probe of quantum phase transitions in topological superconductors

David Nozadze and Nandini Trivedi
*Department of Physics, The Ohio State University,
 191 W. Woodruff Avenue, Columbus, OH 43210, USA*
 (Dated: January 22, 2021)

The non-Abelian statistics of Majorana fermions, their role in topological quantum computation, and the possibility of realizing them in condensed matter systems, has attracted considerable attention. While there have been recent reports of zero energy modes in single particle tunneling density of states, their identity as Majorana modes has so far not been unequivocally established. We make predictions for the local compressibility κ_{loc} , tuned by changing the chemical potential μ in a semiconducting nanowire with strong spin-orbit coupling and in a Zeeman field in proximity to a superconductor, that has been proposed as a candidate system for observing Majorana modes. We show that in the center of the wire, the topological phase transition is signaled by a divergence of κ_{loc} as a function of μ which is an important diagnostic of the topological phase transition. We also find that a single strong impurity potential can lead to a local *negative* compressibility at the topological phase transition. The origin of such anomalous behavior can be traced to the formation of Andreev bound states close to topological phase transitions. Measurable by a scanning electron transistor, the compressibility includes contributions from both single particle states and collective modes and is therefore a complimentary probe from scanning tunneling spectroscopy.

PACS numbers: 71.10Pm, 03.67.Lx, 74.45.+c, 74.90.+n

The search for Majorana fermions in condensed matter systems and their possible application for topological quantum computation¹⁻⁵ has led to several promising proposals for practical realizations of Majorana fermions both in one (1D) and two-dimensional (2D) systems. Majorana fermions can emerge in systems, such as topological insulator-superconductor interfaces^{6,7}, quantum Hall states with filling factor⁴ $5/2$, p -wave superconductors⁸, semiconductor heterostructures^{9,10}, half-metallic ferromagnets^{11,12} and ferromagnetic metallic chains¹³. As shown by Kitaev¹⁴, Majorana fermions can emerge at the ends of 1D spinless p -wave superconducting chain when the chemical potential is in the topological regime.

A realization of the Kitaev chain based on a quantum nanowire made of a semiconductor-superconductor hybrid structure has been proposed^{9,10}. In the presence of Rashba spin-orbit coupling, the parabolic bands for the two spin projections get separated. In addition, a Zeeman field h opens up a gap leading to an effectively spinless 1D system when the chemical potential μ lies in the Zeeman gap. The proximity induced superconductivity with a gap Δ can result in the topological phase^{9,10,15,16}. In this regime, the wire can be realized as a Kitaev chain and should have two Majorana localized zero energy modes at the ends. The nanowire can undergo a quantum phase transition from a topologically trivial superconducting phase to the topological one (or vice versa) by changing the chemical potential or the magnetic field.

There have been recent reports of observations of Majorana fermions in tunneling and the fractional Josephson effect¹⁶⁻¹⁹. Ref. 20 has reported significant progress in creating the Majorana states where spatial location of Majoranas are detected using a scanning tunneling

microscope. All these experimental observations of the existence of Majorana fermions *assume* that the system is in the topological phase and attribute the zero energy density of states to the proposed Majorana modes. However, since there could be several other sources of zero bias anomaly²¹⁻²³, the existence of the Majorana modes has so far not been unequivocally established.

We propose here a definitive method to determine whether or not the nanowire is in the topological or trivial state through measurements of the gate-tuned local compressibility. We find very different behavior of the local compressibility at the edge of the wire and in the center. While the edge harbors Majorana modes which show a zero bias anomaly, the density of states in the center is fully gapped. The compressibility on the other hand shows a sharp singularity in the center of the wire at the topological to trivial phase transitions (see Fig. 1). This is one of our central results. Another key result is that a single impurity can dramatically change the local response: a strong impurity leads to the formation of Andreev bound states and surprisingly this results in a local negative compressibility with a dip at the topological phase transitions as the chemical potential is tuned. An extra peak associated with the bound state appears in the local compressibility above the transition.

Model and methods: We consider a 1D tight-binding Hamiltonian

$$H = - \sum_{i,\sigma} (\mu - V_i) c_{i\sigma}^\dagger c_{i\sigma} - \sum_{i\sigma} t_i (c_{i\sigma}^\dagger c_{i+1\sigma} + \text{h.c.}) + H_{\text{SO}} + H_Z + H_{\text{Int}}, \quad (1)$$

where c_i^\dagger (c_i) is the creation (destruction) operator for an electron on a site i , t_i the nearest-neighbor hop-

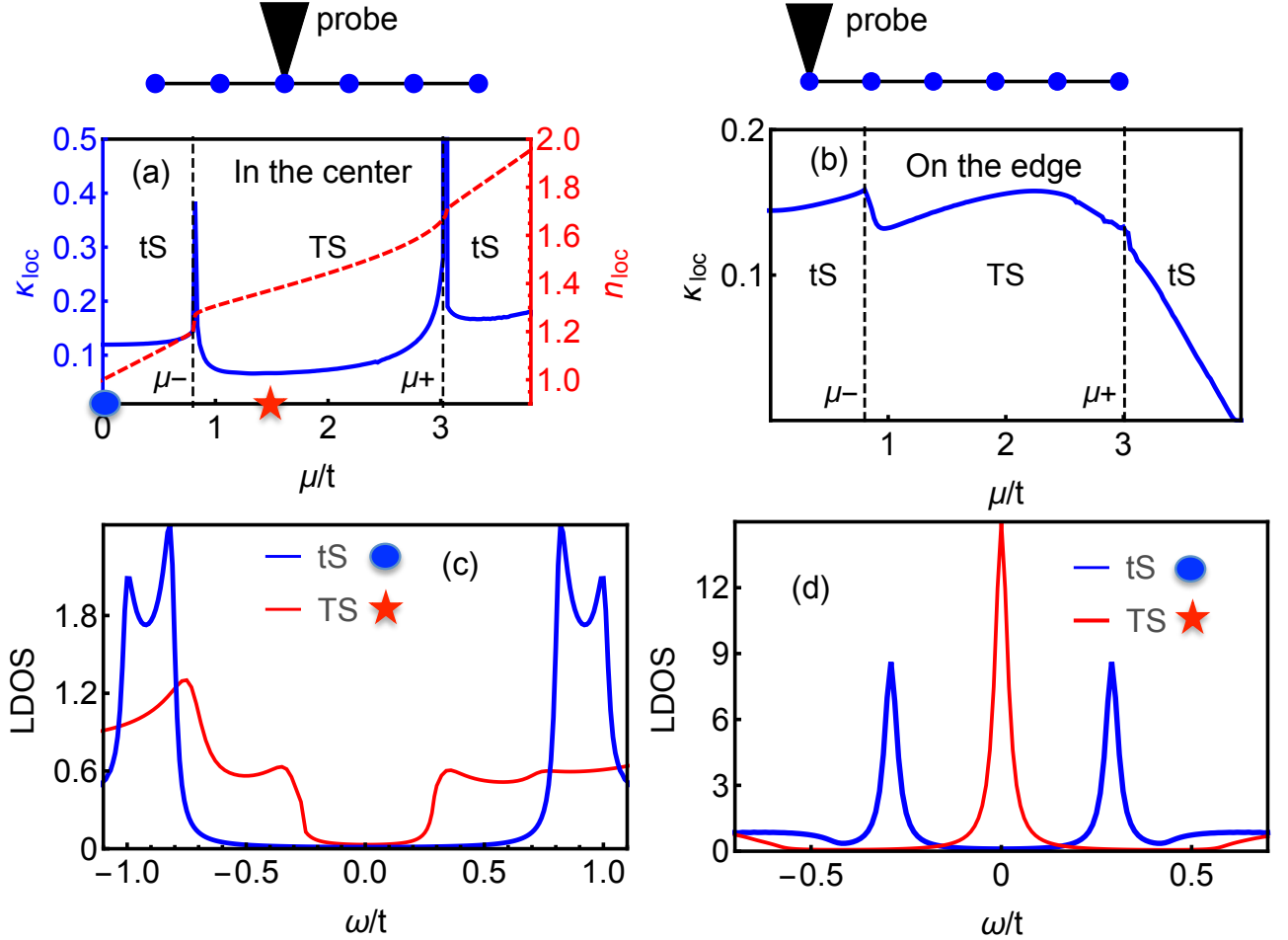


FIG. 1. (Color online). (a) The local particle density n_{loc} (dashed line) and the local compressibility κ_{loc} (solid line) versus the chemical potential μ/t in the center of wire. The compressibility has sharp peaks at the transition between trivial (tS) and topological (TS) superconducting phases. The singularity in κ_{loc} is weakened at the edge of the wire (b). (c,d) The local density of states $N_{\text{loc}}(\omega)$, measured relative to the chemical potential μ , in the trivial ($\mu = 0$, blue circle) and topological ($\mu = 1.5t$, red star) phases. Results presented for chain length $N = 256$ at $T = 0$ with slightly broadened δ -functions in $N_{\text{loc}}(\omega)$.

ping and μ is the chemical potential. The spin-orbit coupling and the Zeeman field terms are given by $H_{\text{SO}} = \frac{1}{2} \sum_{i\sigma} \alpha_i [c_{i+1\sigma}^\dagger (i\sigma_y)_{\sigma\sigma'} c_{i\sigma'} + \text{h.c.}]$ and $H_Z = -h \sum_{i\sigma} c_{i+1\sigma}^\dagger (\sigma_z)_{\sigma\sigma'} c_{i\sigma'}$, respectively. Parameters α_i refer to the Rashba spin-orbit coupling and h to the Zeeman field. V_i is the on-site impurity potential. The interaction term $H_{\text{Int}} = -U \sum_i c_{i\uparrow}^\dagger c_{i\uparrow} c_{i\downarrow}^\dagger c_{i\downarrow}$, where U is the pairing interaction. In the clean limit $\alpha_i = \alpha$, $t_i = t$ and $V_i = 0$.

We solve the model in Eq. (1) within the Bogoliubov-de Gennes (BdG) self-consistent approach and calculate the local particle density n_{loc} and the local density of states $N_{\text{loc}}(\omega)$; (see Supplement for more details). Even though this is a one-dimensional problem we are justified in ignoring the quantum fluctuations, primarily because the system is proximity coupled to a bulk superconductor which damps out the fluctuations.

As shown in Ref. 24, the model in Eq. (1) has

several different phases: trivial superconducting phase (tS), topological superconducting phase (TS) with Majorana fermions at ends of chain, Fulde-Ferrell-Larkin-Ovchinnikov phase (FFLO) with spatially oscillating order parameter Δ and non-zero magnetization, insulator phase (INS) with finite energy gap and normal gas (NG) phase without pairing and energy gap (see Fig. 2 (b)). We are interested in a particular slice of the phase diagram in order to investigate the behavior of the compressibility across the topological to trivial phase transitions. We consider the Zeeman field $h = 1.35t$ and spin-orbit coupling $\alpha = t$ that shows two transitions from the topological to the trivial phases as a function of the chemical potential μ at μ^- and μ^+ . We find the quasiparticle excitation energy $E_{\pm}^2(k) = \epsilon_k^2 + \alpha^2 \sin^2(k) + h^2 + \Delta^2 \pm 2\sqrt{h^2(\epsilon_k^2 + \Delta^2) + \alpha^2 \sin^2(k)\epsilon_k^2}$, where $\epsilon_k = -2t \cos(k) - \mu$. When $h > 0$, the gap ($E_- = 0$) closes at $|\mu^\pm| = (2t \pm \sqrt{h^2 - \Delta^2})$, which cor-

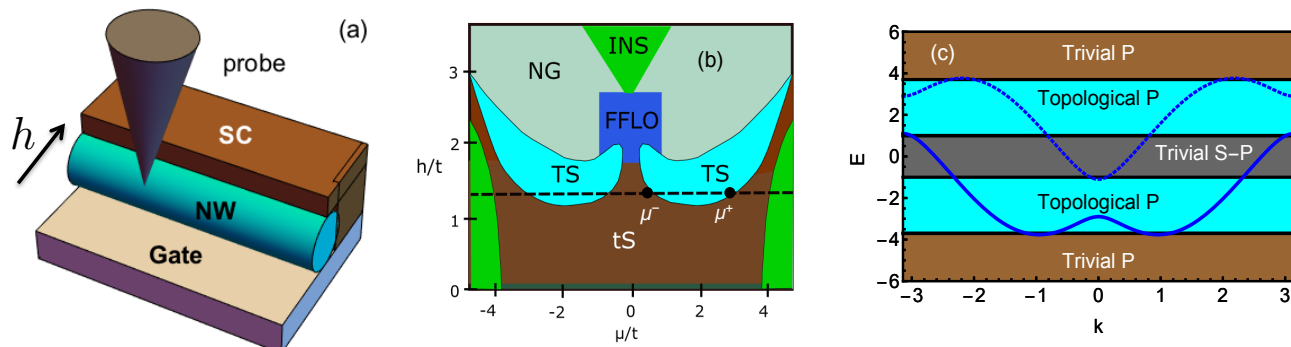


FIG. 2. (Color online). (a) Proposal for measuring local compressibility using an SET (single electron transistor) in the suggested set-up^{9,10} of a nanowire (NW) with spin-orbit coupling in proximity to a superconductor (SC) with an applied magnetic field. (b) Phase diagram of 1D spin-orbit coupled superconductor as function of Zeeman field h/t and the chemical potential μ/t 24. Five different phases can be identified: trivial superconducting (tS), topological superconducting (TS), FFLO, normal gas (NG) and insulator phase (INS). (c) The band structure for a wire with spin-orbit coupling in a magnetic field. As attraction is turned on, different pairing symmetries emerge depending on the location of μ (the Bogoliubov bands have not been shown). Within the first band, the system is described by the Kitaev model that captures the transition from the trivial p to topological p -wave SC. Once the second band is crossed, both interband s -wave and intraband p -wave channels become operative.

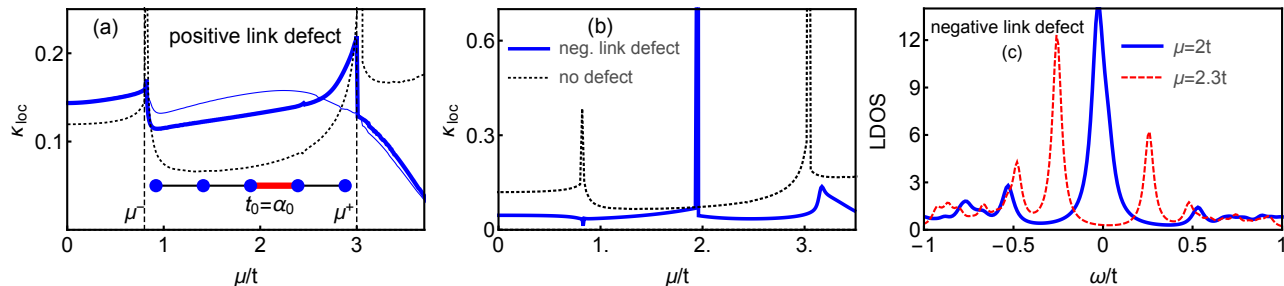


FIG. 3. (Color online). Panels (a,b) The local compressibility κ_{loc} as a function of the chemical potential μ/t for link defects measured on either side of the link. Panel (a) Positive link defect (spin-orbit coupling $\alpha_0 \neq \alpha$ and hopping parameter $t_0 \neq t$ different from the reference values shown for three cases (i) No defect (black dotted line); (ii) $\alpha_0 = t_0 = 0.3t$ (blue thick solid line); (iii) cut wire with $\alpha_0 = t_0 = 0$ (blue thin line). The singularity in κ_{loc} at the topological phase transitions at $\mu = \mu^{\pm}$ is weakened in the presence of the link defect. Panel (b) Negative link defect with $t_0 = -t$ (blue solid line). The sharp peak in κ_{loc} within the topological phase arises because of the formation of a zero-energy bound state on either side of the link defect. (c) Local density of states (LDOS) for a negative link defect showing a bound state at zero energy at $\mu = 2t$ (blue) and away from zero $\mu = 2.3t$ (red).

responds to the phase transitions. The system is in the topological phase when $\mu^- < |\mu| < \mu^+$ and in the trivial phase for $\mu < -\mu^+$ or $\mu > \mu^+$ (see Fig. 2 (c)). For the parameters chosen, $\mu^- \approx 0.84t$ and $\mu^+ \approx 3t$. It is important to note that the system is effectively a “spinless” p -wave superconductor so long as the chemical potential crosses only a single band and the transitions are from the topological phase to a trivial p -wave phase. Once both bands are crossed, the trivial phase has contributions from both s (inter-band) and p -wave (intra-band) pairing channels⁵.

Compressibility at the topological phase transition: From the self consistent BdG solutions of Eq. (1), we obtain the local particle number n_{loc} and its dependence on the global chemical potential μ yields the compressibility $\kappa_{\text{loc}} = \partial n_{\text{loc}} / \partial \mu$. We find that in the center of the

wire the local compressibility shows a logarithmic divergence arising from the gap closing linearly between the topological to the trivial phase transitions (Fig. 1 (a)). In contrast, the singularities are weakened on the edge of the wire (Fig. 1 (b)). It is useful to contrast the compressibility which captures the single particle and the pair (collective modes) density of states (DOS), from the behavior of the single particle density of states $N_{\text{loc}}(\omega)$. As seen in Fig. 1 (c,d), the DOS shows a gap in both the topological and the trivial phases except at the transition where the gap gets closed. However, the compressibility is non-zero in spite of a single-particle gap because of the contribution from the pairs.

This is one of our central results. It highlights the fact that by measuring both the local tunneling DOS at the edge of the wire *and* the local compressibility at the

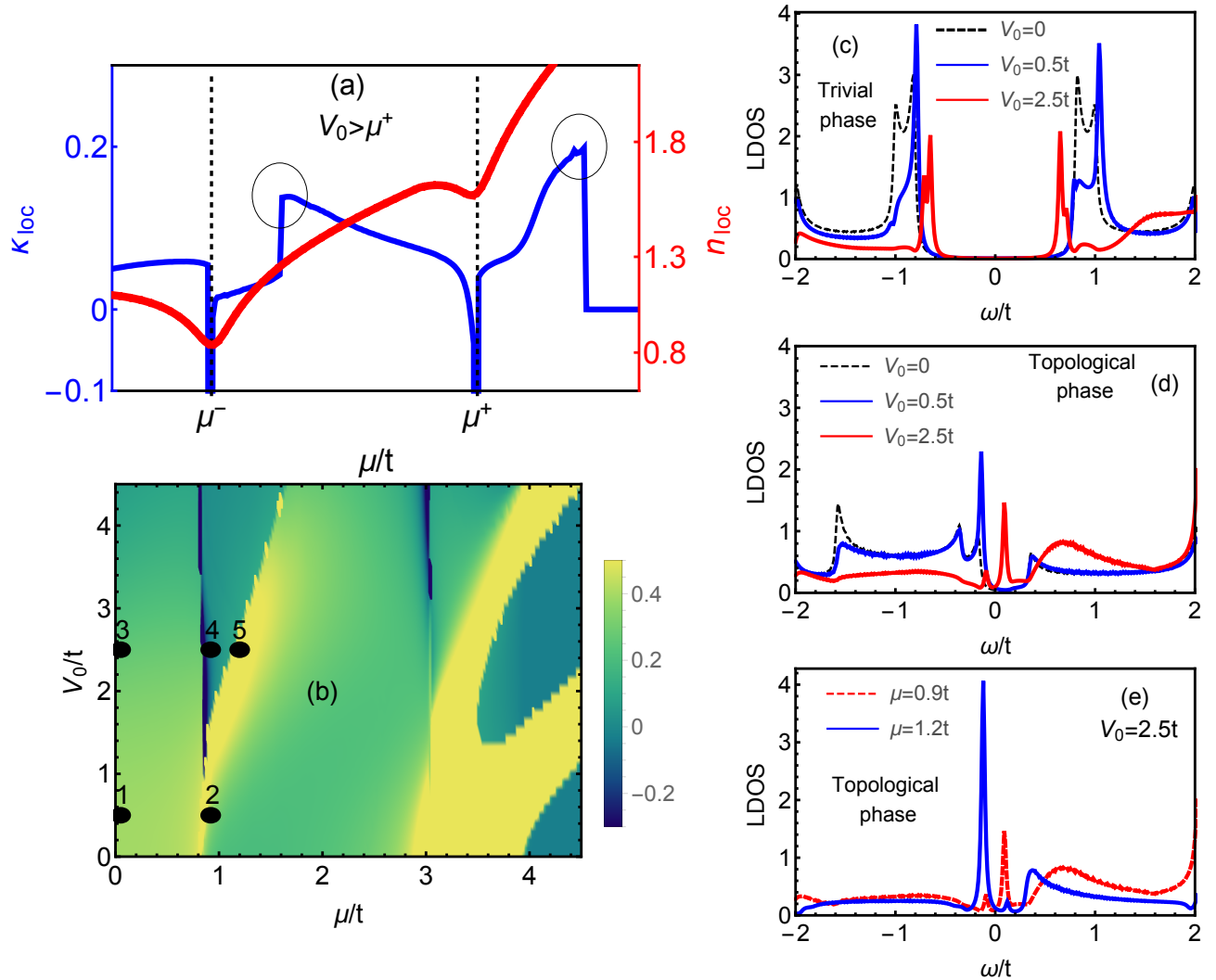


FIG. 4. (Color online). (a) The local particle density n_{loc} and κ_{loc} for a local potential defect $V_0 > \mu^+$. Close to the topological phase transitions $\mu = \mu^\pm$, κ_{loc} becomes negative. In addition, extra peaks (shown by circles) appear in the topological and trivial phases. (b) Density plot of κ_{loc} in the $\mu/t - V_0/t$ plane. (c,d,e) Local density of states for various values of V_0 and μ . (c) shows how a in-gap state appears in the presence of an on-site impurity in the trivial phase ($\mu = 0 < \mu^-$) with s and p wave parings. (d) shows how a non-trivial bound state forms in the topological phase close to the topological phase transition at $\mu = 0.9t > \mu^-$ as impurity strength V_0 increases. The bound state starts to be formed when $V_0 > \mu^-$. (e) The bound state in the topological phase for $\mu = 1.2t$.

center of the wire as a function of μ it is possible to unequivocally determine when the wire is in the topological phase with Majorana modes localized at the edges. As a control, μ can be varied to bring the wire into a trivial phase with a finite compressibility and a gapped single particle DOS.

We next discuss the effect of a weak link and a single potential disorder on the local compressibility.

Weak link: In the presence of a weak link, defined by a hopping $t_0 \neq t$, the local particle number n_{loc} becomes inhomogeneous. We calculate the local compressibility on either side of the link defect $\kappa_{\text{loc}} = \partial n_{\text{loc}} / \partial \mu$ by differentiating it with respect to the global chemical potential μ .

For a positive link defect, i.e. t_0 has the same sign as t , we find that the peaks in the local compressibility are weakened at the transition point (Fig. 3 (a)). In the limit $t_0 = 0$ the wire is cut, the singularity in κ_{loc} is completely suppressed, though the compressibility remains finite. We also consider the case of a link with negative hopping parameter i.e. $t_0 = -t$. Such a negative link can be produced by a local π -junction. The behavior of κ_{loc} as a function of μ is remarkably different from the positive defect. In the topological phase a sharp peak appears in the local compressibility measured on the either side of the link (Fig. 3 (b)) at a particular value of μ_0 ; for the chosen parameters, $\mu_0 = 2t$. This is due to the formation of a zero-energy bound state (Fig. 3 (c)) at μ_0 . It

is important to note that this zero-energy bound state is formed only in the topological phase. At the same time, it does not correspond to a Majorana mode based on the structure and symmetries of the corresponding eigenfunctions (see Supplement for more details). For $\mu \neq \mu_0$ the bound state moves away from zero energy and no longer contributes to the singularity in the compressibility.

Local potential: In the presence of an on-site impurity V_0 , there are several interesting features in the behavior of the local particle density and compressibility as shown in the density plot in Fig. 4 (b).

(i) *Negative local compressibility:* A repulsive potential $V_0 \gtrsim \mu^-$ can have a non-trivial effect on the local density and compressibility. The local particle density is found to *decrease* around the topological phase transition at $\mu = \mu^-$ even as μ increases. Correspondingly, the local compressibility κ_{loc} becomes negative and shows a dip at the transition. For impurity strength somewhat larger than $V_0 \gtrsim \mu^+$, in addition to the dip at $\mu = \mu^-$, a second dip appears at $\mu = \mu^+$ where also the local compressibility κ_{loc} becomes negative (Fig. 4 (a)). The plot for the particle density shown here is schematic for clarity, the actual data with more details can be found in the supplementary information. The reason for the decrease of the local density and the corresponding negative local compressibility is tied to the formation of an impurity bound state (BS) above zero energy that starts to form close to the topological phase transitions.

(ii) *Bound states:* As seen in Fig. 4 (c), In the presence of an on-site impurity, the peaks at the gap edge are suppressed and the gap size is reduced. This can be understood from the fact that the trivial phase has both s and p -wave pairing, and disorder affects the p -wave component more drastically than the s -wave component; however the spectrum remains gapped. In the topological phase where the system is effectively a “spinless” unconventional (p -wave) superconductor, a bound state is formed due to the sign change of the order parameter in this unconventional superconductor.

Figure 4 (d) shows how the zero-energy bound state starts to form when $V_0 \gtrsim \mu^-$. For a fixed V_0 as μ increases, the bound state becomes sharper and moves to zero energy. At this point the zero-energy bound state is detectable as an additional feature shown by a circle

in κ_{loc} (Fig. 4 (a)). With further increase of μ the BS moves below the chemical potential (Fig. 4 (e)). Similarly, a zero-energy BS forms also in the trivial p -wave phase for the impurity strength $V_0 > \mu^+$.

For a negative impurity potential, the BS forms below the Fermi level and more states shift below the Fermi energy to enhance the local density for all μ . In contrast to the scenario of the positive impurity potential, the BS does contribute to the local particle density for a negative impurity. As the result, the local particle density starts to increase as μ decreases, until a sharp BS is formed. This once again causes the local compressibility to become negative around the topological phase transition; (see Supplement for more details).

Conclusions: Our theoretical proposals based on the compressibility, in conjunction with scanning tunneling spectroscopy, are powerful diagnostics for detecting topological phase transitions in 1D spin-orbit coupled superconductors. Specifically in the presence of local defects, the local compressibility can be measured using single-electron transistor (SET) spectroscopies²⁵. Ref. 25 has in fact used the SET in a different context to measure the inverse compressibility locally on a graphene sample as a function of the back-gate voltage or carrier density. We expect the same technique can be applied to the spin-orbit coupled nanowires - superconductor devices to detect the topological phase transition guided by our predictions.

Some of the most promising directions to experimentally investigate are: (a) the sharp peak in the compressibility at the topological phase transition tuned by the Zeeman field in the clean wire, and, (b) the negative compressibility induced by the on-site impurity in the topological phase. In general it will be useful to see the interplay between local scanning and local compressibility spectroscopies for giving insights into single particle and collective modes.

ACKNOWLEDGEMENTS

DN and NT were supported by the NSF under Grant No. NSF-DMR1309461.

¹ C. Nayak, S. H. Simon, A. Stern, M. Freedman, and S. D. Sarma, Rev. Mod. Phys. **80**, 1083 (2008).

² F. Wilczek, Nat. Phys. **5**, 614 (2009).

³ A. Kitaev, Ann. Phys. **303**, 2 (2003).

⁴ G. Moore and N. Read, Nucl. Phys. B **360**, 362 (1991).

⁵ J. Alicea, Rep. Prog. Phys. **75**, 076501 (2012).

⁶ L. Fu and C. L. Kane, Phys. Rev. Lett. **100**, 096407 (2008).

⁷ J. Linder, Y. Tanaka, T. Yokoyama, A. Sudbø, and N. Nagaosa, Phys. Rev. Lett. **104**, 067001 (2010).

⁸ N. Read and D. Green, Phys. Rev. B **61**, 10267 (2000).

⁹ J. D. Sau, R. M. Lutchyn, S. Tewari, and S. D. Sarma, Phys. Rev. Lett. **104**, 040502 (2010).

¹⁰ J. Alicea, Phys. Rev. B **81**, 125318 (2010).

¹¹ M. Duckheim and P. W. Brouwer, Phys. Rev. B **83**, 054513 (2011).

¹² S. B. Chung, H.-J. Zhang, X.-L. Qi, and S.-C. Zhang, Phys. Rev. B **84**, 060510(R) (2011).

¹³ A. C. Potter and P. A. Lee, Phys. Rev. B (2012).

¹⁴ A. Kitaev, Phys. Usp. **44**, 131 (2001).

¹⁵ R. M. Lutchyn, J. D. Sau, and S. D. Sarma, Phys. Rev. Lett. **105**, 077001 (2010).

- ¹⁶ V. Mourik, K. Zuo, S. M. Frolov, S. R. Plissard, E. P. A. M. Bakkers, and L. P. Kouwenhoven, *Science* **336**, 1003 (2012).
- ¹⁷ K. Sengupta, I. Žutić, H.-J. Kwon, V. M. Yakovenko, and S. D. Sarma, *Phys. Rev. B* **63**, 144531 (2001).
- ¹⁸ H.-J. Kwon, V. M. Yakovenko, and K. Sengupta, *Low Temp. Phys.* **30**, 613 (2004).
- ¹⁹ L. P. Rokhinson, X. Liu, and J. K. Furdyna, *Nat. Phys.* **8**, 795 (2012).
- ²⁰ S. Nadj-Perge, I. K. Drozdov, J. Li, H. Chen, S. Jeon, J. Seo, A. H. MacDonald, B. A. Bernevig, and A. Yazdani, *Science* **346**, 602 (2014).
- ²¹ S. Sasaki, S. D. Franceschi, J. M. Elzerman, W. G. van der Wiel, M. Eto, S. Tarucha, and L. P. Kouwenhoven, *Nature* **405**, 764 (2000).
- ²² M. Zareyan, W. Belzig, and Y. V. Nazarov, *Phys. Rev. B* **65**, 184505 (2002).
- ²³ J. D. Sau and E. Demler, *Phys. Rev. B* **88**, 205402 (2013).
- ²⁴ C. Qu, M. Gong, and C. Zhang, *Phys. Rev. A* **89**, 053618 (2014).
- ²⁵ J. Martin, N. Akerman, G. Ulbricht, T. Lohmann, J. H. Smet, K. von Klitzing, and A. Yacoby, *Nat. Phys.* **4**, 144 (2008).

Supplementary Information for: Compressibility as a probe of quantum phase transitions in topological superconductors

David Nozadze and Nandini Trivedi
Department of Physics, The Ohio State University,
191 W. Woodruff Avenue, Columbus, OH 43210, USA

In this supplement, we present: (I) details of the Bogoliubov-de Gennes (BdG) mean field theory for the nanowire in proximity to a superconductor; (II) information about the eigenstates associated with zero-energy bound states that are localized around a negative link (π phase shifted) in the topological phase but are *not* Majorana modes; (III) additional information about the local particle density, local compressibility and the local density of states (LDOS) in the presence of an on-site impurity.

I. Bogoliubov-de Gennes (BdG) approach:

Starting with the full Hamiltonian in Eq. (1) in the main text, we perform a mean-field decomposition of the interaction term in the s -wave local pairing amplitude channel, $\Delta_i = -U \langle c_{i\downarrow}^\dagger c_{i\uparrow}^\dagger \rangle$. In addition, we can add an on-site impurity potential or a weak link. The mean field quadratic Hamiltonian is given by:

$$H = - \sum_{i,\sigma} (\mu - V_i) c_{i\sigma}^\dagger c_{i\sigma} - \sum_{i\sigma} t_i (c_{i\sigma}^\dagger c_{i+1\sigma} + \text{h.c.}) + H_{\text{SO}} + H_Z + \sum_i \Delta_i (c_{i\uparrow}^\dagger c_{i\downarrow}^\dagger + \text{h.c.}). \quad (1)$$

We next diagonalize Eq. (1) using the Bogoliubov transformation $c_{i\sigma} = \sum_n (\gamma_n u_{n\sigma}(i) - \sigma \gamma_n^\dagger v_{n\sigma}(i))$ which leads to BdG equations:

$$\begin{pmatrix} \hat{H}_\uparrow & \hat{\alpha} & 0 & \hat{\Delta} \\ -\hat{\alpha} & \hat{H}_\downarrow & -\hat{\Delta} & 0 \\ 0 & -\hat{\Delta}^* & -\hat{H}_\uparrow & -\hat{\alpha} \\ \hat{\Delta}^* & 0 & \hat{\alpha} & -\hat{H}_\downarrow \end{pmatrix} \begin{pmatrix} u_{n\uparrow}(j) \\ u_{n\downarrow}(j) \\ -v_{n\uparrow}(j) \\ v_{n\downarrow}(j) \end{pmatrix} = E_n \begin{pmatrix} u_{n\uparrow}(j) \\ u_{n\downarrow}(j) \\ -v_{n\uparrow}(j) \\ v_{n\downarrow}(j) \end{pmatrix} \quad (2)$$

where the excitation eigenvalues $E_n \geq 0$. Here $\hat{H}_\sigma u_{n\sigma}(i) = (-\mu \pm h + V_i) u_{n\sigma}(i) - t_i (u_{n\sigma}(i+1) + u_{n\sigma}(i-1))$, $\hat{\alpha} u_{n\uparrow}(i) = \alpha (u_{n\downarrow}(i-1) - u_{n\downarrow}(i+1))$ and $\hat{\Delta} u_{n\sigma}(i) = \Delta_i u_{n\sigma}(i)$. In terms of the eigenfunctions of the BdG hamiltonian, the local pairing amplitudes and local densities are given by:

$$\Delta_i = -U \sum_{E_n \geq 0} u_{n\uparrow}(i) v_{n\downarrow}(i) \tanh(E_n/2T). \quad (3)$$

and

$$n_i = \frac{1}{2} \sum_{n,\sigma} [|u_{n\sigma}(i)|^2 f(E_n) + |v_{n\sigma}(i)|^2 (1 - f(E_n))] , \quad (4)$$

where $f(E_n)$ is the Fermi function. The solutions of the BdG equations are iterated until self consistency is achieved at each site. In these studies we have set $T = 0$. In the problem at hand, since the pairing in the nanowire is imposed by proximity with a bulk superconductor, it may be not necessary to obtain the pairing amplitudes self consistently, however in the presence of disorder (site or link), the self consistency becomes more relevant and is included in our investigation.

Once self consistency is achieved the single-particle density of states is obtained from

$$N_i(\omega) = \sum_{n,\sigma} [|u_{n\sigma}(i)|^2 \delta(\omega - E_n) + |v_{n\sigma}(i)|^2 \delta(\omega + E_n)] . \quad (5)$$

In the text the local density from Eq. (4) is denoted by n_{loc} and the local single-particle density of states by $N_{\text{loc}}(\omega)$.

II. Zero-energy bound state due to a weak link:

As shown in the main text a negative link impurity $t_0 = -t$ induces zero-energy bound states in the topological phase. Are these Majorana modes or simply Andreev bound states? In order to get some insight about these modes we look at the corresponding eigenfunctions $u_\sigma(i)$ and $v_\sigma(i)$. As seen in the Fig. 1 (a), close to link impurity, the eigenstates do not satisfy the symmetry conditions $u_\sigma(i) = v_\sigma^*(i)$ or $u_\sigma(i) = -v_\sigma^*(i)$ that is required for a Majorana mode (Fig. 1 (b)). Thus, even though these two zero-modes are in the topological phase these are not Majorana modes.

III. Local particle density and compressibility:

We present here the actual data in Fig. 2 of the supplement for the local particle density and the local compressibility in the presence of an on-site impurity potential $\mu^+ > V_0 > \mu^-$, corresponding to Fig. 4 (a) of the main text. Close the topological phase transition at $\mu = \mu^- = 0.84t$, the local particle density starts to decrease even as the chemical potential increases and the local compressibility κ_{loc} becomes negative (Fig. 2 (a,b)). Also, an extra peak appears in κ_{loc} in the topological phase (Fig. 2 (b)) due to the formation of an Andreev bound state as explained in main text. For an on-site impurity potential $V_0 > \mu^+$, close the topological phase transitions $\mu = \mu^\pm = 3t$, the local particle density once again starts to decrease as the chemical potential increases and local compressibility becomes negative (Fig. 2 (c,d)). The additional extra peak in the compressibility now appears in the trivial phase in addition

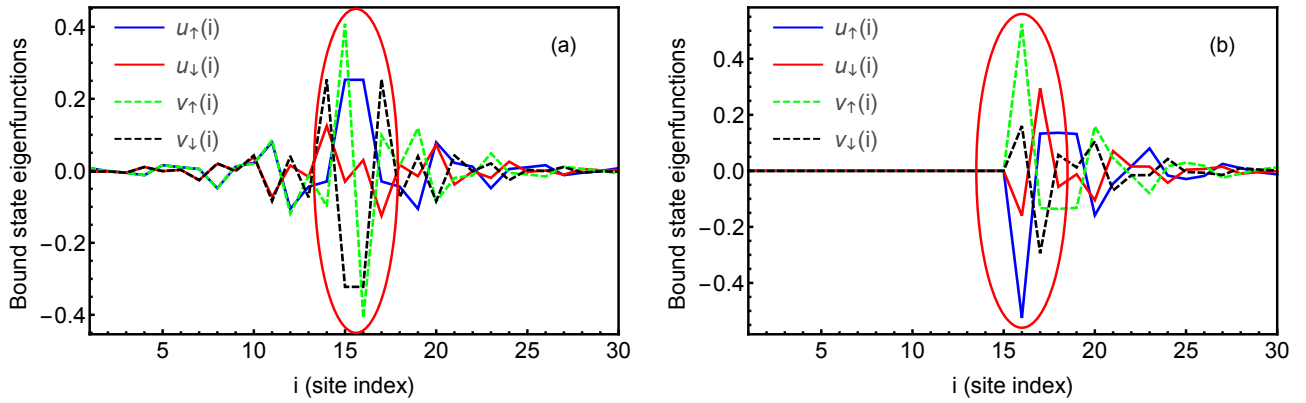


FIG. 1. (Color online). (a) The bound state eigenfunctions at zero-energy in the presence of a negative link impurity $t_0 = -t$ between sites 15 and 16. (b) The bound state eigenfunctions at zero-energy for a broken link $t_0 = \alpha = 0$ between sites 15 and 16. From the symmetry conditions $u_\sigma(i) = -v_\sigma(i)$ required for a Majorana fermion, it is evident that while the bound state in (b) is a Majorana bound state that is topologically protected to be at zero energy, the bound state in (a) is an Andreev bound state that happens to be at zero energy. The system size $N = 256$, and parameters $\alpha = t$, $h = 1.35t$ at $T = 0$.

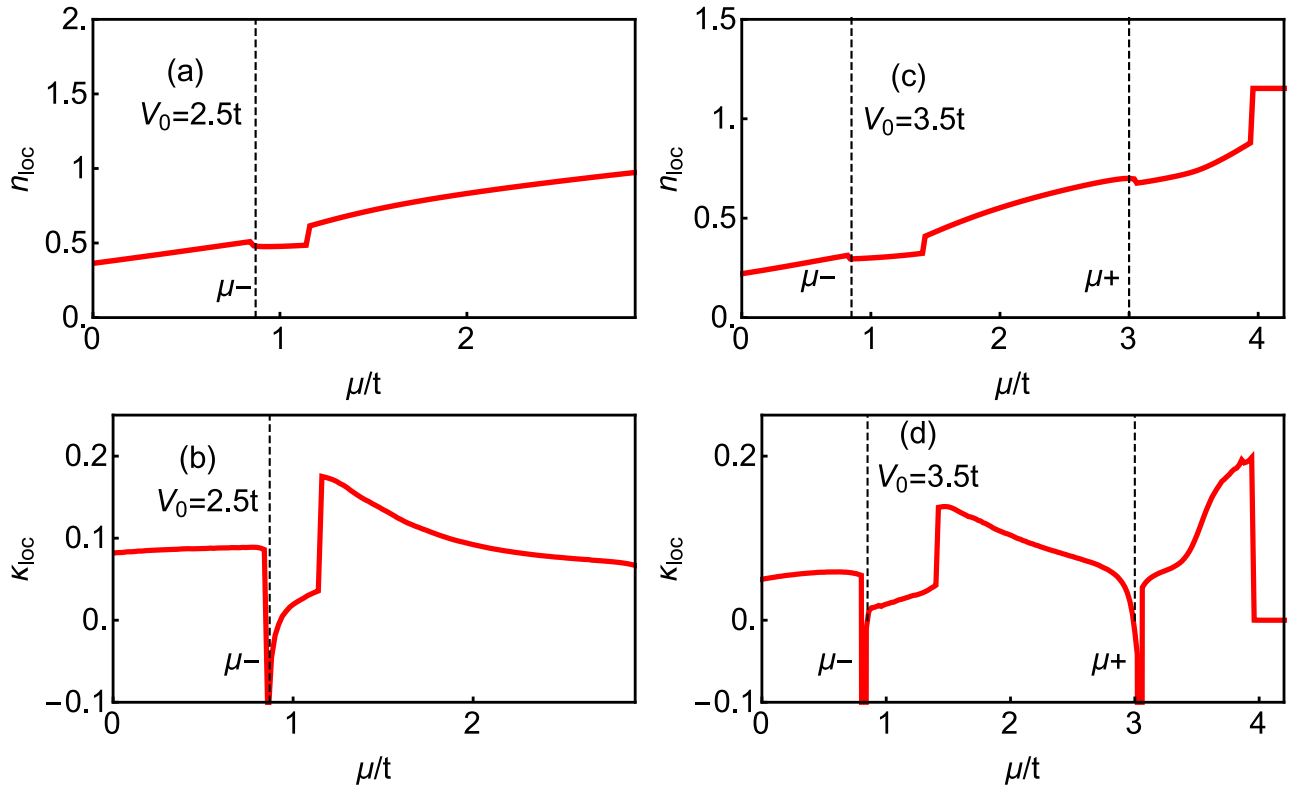


FIG. 2. (Color online). The local particle density n_{loc} and the compressibility κ_{loc} versus chemical potential μ/t for two values of the on-site impurity potential V_0 .

to peak in the topological phase (Fig. 2 (d)), once again arising because of an Andreev bound state.

As discussed in the main text, we discussed the role of an Andreev the bound in the presence of an on-site impurity potential and how that results in a decrease of the particle density with increasing μ . This was shown previously in the LDOS for a positive potential $V_0 >$

0. Here, we present the results for the LDOS in the presence of a negative potential $V_0 < 0$. In the latter case, the local particle density starts to *increase* as the μ increases because the bound state now forms *below* the Fermi level so more states shift below the Fermi level (Fig. 3). Thus in contrast to the scenario of the positive impurity potential, the bound state *does* contribute to the local particle density for a negative on-site impurity.

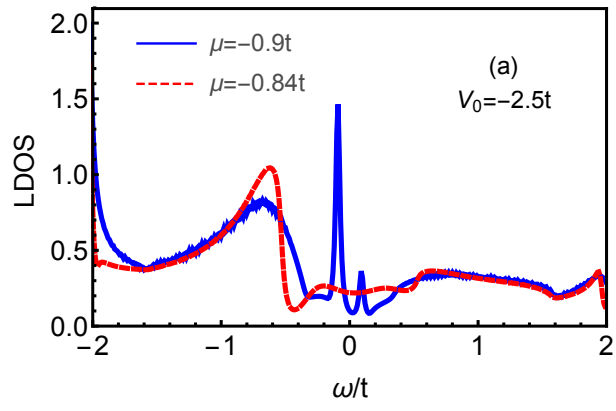


FIG. 3. (Color online). Formation of the bound state close to the topological phase transition for a negative on-site potential.